Published in final edited form as:
Neuroimage. 2011 April 01; 55(3): 880–90. doi:10.1016/j.neuroimage.2010.12.008.

DTI measures in crossing-fibre areas: Increased diffusion anisotropy reveals early white matter alteration in MCI and mild Alzheimer's disease

Gwenaëlle Douaud[a,*], **Saâd Jbabdi**[a], **Timothy E.J. Behrens**[a], **Ricarda A. Menke**[a], **Achim Gass**[b], **Andreas U. Monsch**[c], **Anil Rao**[d], **Brandon Whitcher**[d], **Gordon Kindlmann**[e], **Paul M. Matthews**[d], **Stephen Smith**[a]

[a]FMRIB Centre, University of Oxford, UK [b]Departments of Neurology and Neuroradiology, University Hospital, Basel, Switzerland [c]Memory Clinic, Department of Geriatrics, University Hospital, Basel, Switzerland [d]GlaxoSmithKline, Clinical Imaging Centre, Hammersmith Hospital London, UK [e]Department of Computer Science and Computation Institute, University of Chicago, USA

Abstract

Though mild cognitive impairment is an intermediate clinical state between healthy aging and Alzheimer's disease (AD), there are very few whole-brain voxel-wise diffusion MRI studies directly comparing changes in healthy control, mild cognitive impairment (MCI) and AD subjects. Here we report whole-brain findings from a comprehensive study of diffusion tensor indices and probabilistic tractography obtained in a very large population of healthy controls, MCI and probable AD subjects. As expected from the literature, all diffusion indices converged to show that the cingulum bundle, the uncinate fasciculus, the entire corpus callosum and the superior longitudinal fasciculus are the most affected white matter tracts in AD. Significant differences between MCI and AD were essentially confined to the corpus callosum. More importantly, we introduce for the first time in a degenerative disorder an application of a recently developed tensor index, the “mode” of anisotropy, as well as probabilistic crossing-fibre tractography. The mode of anisotropy specifies the type of anisotropy as a continuous measure reflecting differences in shape of the diffusion tensor ranging from planar (e.g., in regions of crossing fibres from two fibre populations of similar density or regions of “kissing” fibres) to linear (e.g., in regions where one fibre population orientation predominates), while probabilistic crossingfibre tractography allows to accurately trace pathways from a crossing-fibre region. Remarkably, when looking for whole-brain diffusion differences between MCI patients and healthy subjects, the only region with significant abnormalities was a region of crossing fibres in the centrum semiovale, showing an increased mode of anisotropy. The only white matter region demonstrating a significant difference in correlations between neuropsychological scores and a diffusion measure (mode of anisotropy) across the three groups was the same region of crossing fibres. Further examination using probabilistic tractography established explicitly and quantitatively that this previously unreported

[*]Corresponding author. FMRIB Centre, John Radcliffe Hospital, Headley Way, OX3 9DU, Oxford, UK. Fax: +44 1865 222 717. douaud@fmrib.ox.ac.uk.

Europe PMC Funders Author Manuscripts

increase of mode and co-localised increase of fractional anisotropy was explained by a relative preservation of motor-related projection fibres (at this early stage of the disease) crossing the association fibres of the superior longitudinal fasciculus. These findings emphasise the benefit of looking at the more complex regions in which spared and affected pathways are crossing to detect very early alterations of the white matter that could not be detected in regions consisting of one fibre population only. Finally, the methods used in this study may have general applicability for other degenerative disorders and, beyond the clinical sphere, they could contribute to a better quantification and understanding of subtle effects generated by normal processes such as visuospatial attention or motor learning.

Introduction

More than 35 million people will be suffering from dementia in 2010 (World Alzheimer report 2009, http://www.alz.co.uk/research/worldreport) but a clinical diagnosis of Alzheimer's disease (AD) can only be made after development of disabling dementia (Cedazo-Monguez and Winblad, 2010; Hess, 2009). On the other hand, mild cognitive impairment (MCI) is an intermediate clinical state between the cognitive changes of aging and the earliest clinical manifestations of AD (Petersen, 2009), with more than half of the MCI population progressing to dementia within 5 years (Gauthier et al., 2006). However, all population-based studies to date have found MCI to be highly heterogeneous (Ganguli, 2006). There is therefore a crucial need for techniques that would permit to stratify MCI and AD patients, to better understand the progression of the disease and to establish a prognosis.

Diffusion magnetic resonance imaging provides insight into white matter connectivity and microstructural integrity. Interestingly, one study in AD patients showed a focal loss of white matter volume in the parahippocampal region, whereas changes detected using diffusion images were widespread and extended beyond the medial temporal lobe (Serra et al., 2010). It is therefore likely that diffusion imaging is more sensitive to detect white matter alterations before this microstructural change develops into macrostructural loss of white matter measurable by analyses such as voxel-based morphometry.

However, despite a rich literature on diffusion tensor imaging in MCI and AD (reviews in Bozzali and Cherubini, 2007; Chua et al., 2008; Hess, 2009), there have been few wholebrain voxel-wise studies in which no a priori hypothesis was made regarding anatomical localisation of white matter abnormalities (e.g. Rose et al., 2006; Teipel et al., 2007; Stricker et al., 2009). Particularly, to our knowledge only three such studies examined healthy elderly, MCI and AD populations together, with quite limited population samples (Medina et al., 2006; Serra et al., 2010; Liu et al., 2009).

Our initial aim was to investigate whole-brain white matter microstructural abnormalities in a very large diffusion study including healthy control participants, MCI and AD patients. For this purpose, we used Tract-Based Spatial Statistics (TBSS), a voxel-wise method which increases the sensitivity and the interpretability of the results in a context of neurodegenerative disorders such as AD, when there might be some substantial structural changes and hence cross-subject misalignments (Smith et al., 2006).

Europe PMC Funders Author Manuscripts

Europe PMC Funders Author Manuscripts

To answer some specific questions that arose in the course of this clinical study, we came to use for the first time in a degenerative disorder a recently developed tensor index, the "mode" of anisotropy (Ennis and Kindlmann, 2006) and a new feature of probabilistic tractography (Behrens et al., 2007). The mode of anisotropy specifies the type of anisotropy as a continuous measure reflecting differences in shape of the diffusion tensor ranging from planar (e.g., in regions of crossing fibres from two fibre populations of similar density) to linear (e.g., in regions where one fibre population orientation predominates), while probabilistic crossing-fibre tractography permits to accurately trace pathways from a crossing-fibre region.

Materials and methods

This imaging study was part of the EAGLE (Early Alzheimer's disease Genetics — A Longitudinal Evaluation) study and was approved by the Ethics Committee of Both Basel (Switzerland). All subjects gave written informed consent.

Subjects

170 participants took part in this study (61 normal controls [CON], 56 MCI patients and 53 probable AD patients without a vascular component). For all subjects, comprehensive neuropsychological data and CSF concentrations of tau, phosphorylated tau and β-amyloid were collected (for more details, see Supplementary material and supplementary Tables S1 and S2).

Criteria for CON included (i) performance within normal limits on the comprehensive neuropsychological assessment, (ii) no past or current neurological or psychiatric disorders, (iii) normal neurological and general medical examination and (iv) living independently in the community. MCI subjects were diagnosed according to the criteria by Winblad and colleagues (Winblad et al., 2004). The diagnosis of AD was made when both the DSM-IV criteria (American Psychiatric Association, 1994) and the NINCDS-ADRDA criteria (McKhann et al., 1984) were fulfilled.

50 patients had amnestic MCI (2 single domain, 48 multi-domain) and 6 patients had non-amnestic MCI (3 single domain, 3 multidomain) (Winblad et al., 2004). 54 MCI patients had an MMSE ≥ 25. 50 patients had mild probable AD (MMSE ≥ 20) and 3 had mild-to-moderate probable AD (18 ≤ MMSE b 20).

All participants but five were followed up for at least one year to confirm the diagnosis and determine if any of the subjects made the transition to another diagnosis. All of the normal controls and AD patients remained as such. 3 MCI patients reverted to control status (MCI is indeed an unstable and heterogeneous entity with a far wider range of outcomes than in the clinical setting, including reversion to normal in a substantial proportion, Ganguli, 2006), one MCI patient made a transition to dementia with Lewy bodies and 7 MCI patients made the transition to AD, in good accordance with a rate of conversion to AD of ~10–16% observed per year in other studies (Grundman et al., 2004; Petersen et al., 2005; Gauthier et al., 2006). All of these patients whose diagnosis evolved over the one year follow-up period were considered in this cross-sectional study as MCI patients.

Data acquisition

The 170 participants underwent the same imaging protocol including whole-brain diffusion-weighted scanning using a 3 T Allegra MR imager (Siemens, Erlangen, Germany) with a standard quadrature head coil and maximum 40 mT.m−1 gradient capability. Diffusion-weighted images were obtained using echo-planar imaging (SE-EPI, TE/TR=89/7000ms, 54 axial slices, bandwidth=2056Hz/vx, voxel size 2.5 × 2.5 × 2.5 mm3) with 30 isotropically distributed orientations for the diffusion-sensitising gradients at a b-value of 900 s mm−2 and 6 b = 0 images. To increase signal-to-noise ratio, scanning was repeated twice and both scans were corrected for head motion and eddy currents using affine registration before being combined.

Image processing

Voxel-wise analyses of tensor indices—Fractional anisotropy (FA), mean diffusivity (MD) and mode of anisotropy (MO) maps were generated from a tensor-model fit in FSL (Smith et al., 2004). The mode of anisotropy specifies the type of anisotropy and gives complementary information to FA, as it is mathematically orthogonal to it (Ennis and Kindlmann, 2006). It varies from −1 to +1 as the type of anisotropy (or shape of the diffusion tensor) ranges from planar (i.e. disc-like $\lambda 1 \sim \lambda 2$ N $\lambda 3$: the second eigenvalue is close to the first, for instance in areas of crossing fibres with two roughly equal fibre populations or areas of “kissing” fibres) to linear (i.e. cigar-like $\lambda 1$ N $\lambda 2 \sim \lambda 3$: the second eigenvalue is close to the third, for example in areas where one fibre population predominates).

Voxel-wise differences in DTI indices were assessed using TBSS in FSL which increases the sensitivity and the interpretability of the results compared with voxel-based approaches based purely on non-linear registration (Smith et al., 2006). TBSS aims to solve the problematic issues of simple voxel-wise methods via the use of a carefully tuned non-linear registration (Andersson et al., personal communication), followed by the projection of the nearest maximum FA values onto a skeleton derived from the mean FA image. This projection step aims to remove the effect of cross-subject spatial variability that remains after the non-linear registration.

Because of substantial ventricular enlargement that was seen in many subjects in this study, we created a study-specific FA template by non-linearly registering all native-space FA images to an FA template in the MNI space (www.fmrib.ox.ac.uk/fsl/data/FMRIB58_FA) and subsequently averaging them. Then, we non-linearly registered the original FA scans to this study-specific FA template. The resulting warpfields were then applied to both MD and MO images.

Finally, because we found an increase of MO in AD patients compared with healthy controls in regions of crossing fibres that the TBSS skeleton does not entirely investigate (as these crossing fibres can lead to a substantial drop of FA in the template), we looked at voxel-wise, as opposed to “skeletonised”, MO and FA values in these regions. For this voxel-wise analysis, we took the MO and FA maps registered to the standard space as described above and, instead of “skeletonising” these images, we convoluted them with a Gaussian kernel (σ

= 1 mm). The hypothesis was that the MO increase (demonstrating a transition to more linear diffusion tensor in the white matter) might reflect a selective degeneration of one fibre population amongst the crossing fibres at this level: either the cognitive-related association fibres running antero-posteriorly and medio-laterally (superior longitudinal fasciculus) or the motor-related projection fibres running dorsoventrally (corticospinal/corticopontine tracts and superior thalamic radiation). We should first be able to confirm this theory with a co-localised increase of FA, increase that has been previously shown to characterise a selective degeneration in crossing fibre region (Douaud et al., 2009). Second, if an increase of FA were indeed found, our hypothesis was that we should be able to attribute it even more specifically to a relative preservation of the motor-related projection fibres (compared with the association fibres) using a probabilistic tractography approach (Behrens et al., 2007).

Probabilistic tractography from crossing fibres region—Seeding the tractography algorithm explicitly from a region of crossing fibres (defined by the significant increase of FA in the centrum semiovale) is a challenging procedure as any slight shift of the region of interest (ROI) could lead into dramatic change in the outcome of the tractography. For that reason, we carefully selected a subsample of 15 healthy controls and 15 AD patients (matched for age and gender) displaying only mild to moderate deformation of the brain, as measured by the average displacement across all brain voxels generated by the non-linear warping. Importantly, these subjects were clinically representative of each corresponding group (see Table S1 of the Supplementary material) and exhibited the same micro- structural abnormalities (data not shown).

We fitted a multi-fibre diffusion model (Behrens et al., 2007) that estimates probability distributions on the direction of 1 or more fibre populations at each brain voxel in the diffusion space of each subject. The algorithm was restricted to estimating two fibre orientations at each voxel, because of the limited b value and number of gradient orientations in the diffusion data. To be able to perform the probabilistic tractography in the standard space for each of the 30 subjects, we fed both the warpfields generated as described above during the first steps of TBSS and their corresponding inversed warpfields into the tractography algorithm. Tractography was then performed in standard space from every voxel of the same seed ROI for all subjects to trace two different pathways: the association fibres and the projection fibres running through this ROI (Wedeen et al., 2008).

To identify these two fibre populations, we defined “target” regions as well as “exclusion” areas in the standard space, avoiding in this way a possible bias related to the creation of individual ROIs. For the association fibres, we drew four planar target regions in the medio-lateral direction (x = 22; x = 27; x = 63; x = 68) and for the projection fibres, three planar regions in the dorso-ventral direction (z = 63; z = 39; z = 31) (Fig. 1). The exclusion mask for the association fibres consisted of the target mask for the projection fibres and vice-versa (Fig. 1). In both cases, we added a mid-sagittal callosal area to the exclusion mask, and to the exclusion mask for the association fibres, we added a fourth planar region (z = 43) while a planar region in the antero-posterior direction was added to the exclusion mask for the projection fibres (y = 85). For each tractography, we then generated 5000 samples (or “particles”) from each seed voxel to build up a connectivity distribution and only those that passed through the target mask and none of the regions of the exclusion mask were retained.

As our seed ROI was an area of crossing fibres, these 5000 particles were initially sampled equally amongst both estimated fibre orientations. Finally, we counted for each subject the average number of particles within the crossing fibre ROI which "belonged" to the association fibres and to the projection fibres and calculated the ratio of the two.

Statistical analyses—To achieve accurate inference in our voxel-wise analyses, including full correction for multiple comparisons over space, we used permutation-based nonparametric inference within the framework of the general linear model (5000 permutations) (Nichols and Holmes, 2002). For our model we further split the three diagnosis groups (CON, MCI, AD) according to gender, giving six group means in our statistical design. Permutations were only carried out between groups of the same gender. This allowed us to statistically account for the difference in gender ratio across groups. We first looked for significant abnormalities across the three diagnosis groups using an F-test. We also tested whether adding the age as a nuisance covariate or excluding the 8 MCI patients who later went on to convert to AD and dementia with Lewy bodies would change the spatial pattern of the results. Second, we tested for significant diffusion differences for six post-hoc contrasts (CON-AD, CON-MCI, MCI-AD, AD-CON, MCI-CON, AD-MCI). We were also interested in looking at white matter regions that would specifically discriminate the three groups by showing differences in correlations with neuropsychological scores (i.e. differences in slopes). We therefore focused on the interaction effect between diagnosis and neuropsychological scores using the same six contrasts as described above. TBSS results for FA, MD and MO were considered significant for P b 0.05, corrected for multiple comparisons using the "2D" parameter settings with threshold-free cluster enhancement (TFCE), a method which avoids using an arbitrary threshold for the initial cluster-formation (Smith and Nichols, 2009). Voxel-wise (as opposed to "skeletonised") results of MO were considered significant for P b 0.05, corrected for multiple comparisons using the "3D" parameter settings for TFCE. We restrained the voxel-wise analysis of FA to areas of significant increase of MO. Again, results were considered significant for P b 0.05 (TFCE-corrected).

Differences between the number of particles belonging to the association fibres, the projection fibres and the ratio of these two were assessed using a one-tail t-test as we had a priori hypotheses on the direction of the effect. Tractography results were considered significant for Pb0.05.

Results

Whole-brain characterisation of the diffusion abnormalities across the three groups

Fractional anisotropy and mean diffusivity group comparison results—Using an F-test, we found significant FA and MD differences across the three groups mainly bilaterally in the corpus callosum from genu to splenium, in the anterior commissure, the external/extreme capsule/ temporal stem (presumably in the uncinate fasciculus as described in Kier et al., 2004), the cingulum bundle (dorsal and posterior part), the superior longitudinal fasciculus (SLF) and in the centrum semiovale (Fig. 2, Figs. S1 and S2 of the Supplementary material). MD differences across the three groups also extended in the

anterior thalamic radiation. Adding the age as a nuisance covariate or excluding the 8 MCI patients whose diagnosis changed after one year did not change the spatial pattern of the results (Figs. S4, S5 and S6 of the Supplementary material). Inside the region of interest defined by the significant TBSS results, we found that the primary distinction of FA and MD values was between the controls and the AD patients, as the MCI patients and healthy controls had similar values (Fig. 2).

Only the post-hoc contrasts where AD patients showed lower FA and higher MD than MCI patients and where AD patients showed lower FA and higher MD than controls were significant after correction for multiple comparisons (Fig. 3). Lower FA and higher MD values in the AD patients were almost entirely confined to the corpus callosum when contrasted with MCI patients. On the contrary, AD patients had widespread lower FA and higher MD than the controls mainly in the corpus callosum, in the anterior commissure, in the uncinate fasciculus, in the cingulum bundle and in the SLF (and extended in the centrum semiovale only for MD values). We found no significant differences between controls and MCI patients (Table 1).

Mode of anisotropy group comparison results—We found widespread significant MO differences across the three groups, mainly bilaterally in the corpus callosum (from genu to splenium), in the anterior commissure, in the external/extreme capsule/temporal stem (presumably the uncinate fasciculus), in the cingulum bundle (dorsal and posterior part), in the centrum semiovale and in the SLF (Fig. 4, Fig. S3 of the Supplementary material).

Remarkably, all group-difference contrasts were significant after correction for multiple comparisons except that controls did not have significantly higher MO than MCI patients. AD patients had significantly lower MO values than MCI patients or controls mainly in the corpus callosum and the cingulum bundle, with also significantly lower MO values in the SLF when contrasted with controls (Fig. 5).

The opposite contrasts, showing an MO increase with disease, strikingly proved to be significant as well. Sensitivity to CON-MCI differences was therefore higher using MO than with FA or MD. Particularly, we found significantly higher MO values in the MCI patients compared with the control participants in the centrum semiovale (Fig. 6, Table 1), in regions of crossing fibres (Wedeen et al., 2008).

Correlations with neuropsychological scores—Neuropsychological assessments including the MMSE, categorical verbal fluency (animals), phonological verbal fluency (S words), the Boston naming test and the Trail Making test discriminated between the three groups (see Table S2 of the Supplementary material).

We found significant differences across groups in the correlations between diffusion indices and neuropsychological scores (i.e. a significant difference in the slopes between groups) for the mode of anisotropy and the MMSE (AD vs. MCI) or the Trail making test part A (CON vs. MCI and CON vs. AD), as well as for the mean diffusivity and the Boston naming test (CON vs. MCI). Notably, all of the differences in correlations were located in the same

region of crossing fibres in the centrum semiovale as identified for differences in mode of anisotropy across groups (Fig. 4) and also extended to the SLF for the differences between mean diffusivity and Boston naming test scores (Fig. S7 of the Supplementary material).

Focusing on the crossing-fibre region in the centrum semiovale: a selective preservation of the motor-related pathways?—To further explore the genesis of the structural changes underlying the results in the region of crossing fibres, we performed a voxel-wise (as opposed to TBSS skeletonised) analysis which showed an increase of MO in AD patients compared with controls that was highly significant and located in the centrum semiovale. When looking at a possible concurrent increase of FA in this voxel-wise region specifically, we found significantly higher FA values in the AD patients than in the controls (Fig. 7). Anatomically, this increase was located in a region of crossing fibres between the ascending/ descending motor-related projection tracts (essentially corticospinal tract) and the association pathways (essentially SLF), as identified from the Jülich cytoarchitectonic atlas (www.fmrib.ox.ac.uk/fsl/data/atlas-descriptions).

To confirm this, we used the region of significant increase of FA as a seed for tractography. From this seed, we were able to successfully reconstruct both projection fibres and association fibres in a comparable, anatomically relevant way for each of the healthy and AD subjects (Fig. 8). The projection fibres encompassed the corticospinal/corticopontine tracts and the superior thalamic radiation, while the association fibres were constituted essentially of the SLF.

We found a highly significant decrease of particles belonging to the association fibres in the AD patients ($P = 0.0002$), while no significant difference was found for the projection fibres ($P = 0.217$) (Fig. 8). The ratio of particles belonging to projections fibres/association fibres was significantly increased in the AD patients relative to healthy controls ($P = 0.002$) (Fig. 8). In two separate ROIs consisting of the average reconstructed association fibres and projection fibres respectively, we further demonstrated an increase of the uncertainty on the estimated orientation of the main fibre population in the association fibres ($P = 0.0168$), no significant difference in the projection fibres ($P = 0.378$) and a significant interaction between association fibres/ projection fibres and the diagnosis group ($P=0.0157$).

Discussion

Whole-brain voxel-wise studies studying control, MCI and AD participants together are sparse (Medina et al., 2006; Serra et al., 2010; Liu et al., 2009). Here, we first report whole-brain findings from a comprehensive study of diffusion tensor indices and probabilistic tractography obtained in a very large population of healthy, MCI and AD subjects. As expected from the literature (reviews in Chua et al., 2008; Hess, 2009), all indices converged to demonstrate white matter microstructural changes in the cingulum bundle, uncinate fasciculus, corpus callosum, anterior commissure and SLF in patients with AD. MCI patients showed intermediate differences between healthy controls and AD patients – though closer to the healthy group – with significant differences between MCI and AD essentially confined to the corpus callosum. But more interestingly, when looking for whole-brain diffusion differences between MCI patients and healthy subjects, the only region where we

found significant abnormalities was a region of crossing fibres in the centrum semiovale, showing an increase of mode of anisotropy, a recently developed tensor index (Ennis and Kindlmann, 2006). A voxel-wise analysis of white matter FA confirmed differences in the same region, showing an atypical higher FA in the patient group than in healthy controls. We later demonstrated using quantitative crossing-fibre tractography that the previously unreported increase of mode and fractional anisotropy in this region was related to a selective sparing of the motor-related projection fibres crossing the affected association fibres of the SLF. Together these results illustrate the sensitivity of diffusion MRI to changes in white matter microstructure in AD and more remarkably in MCI, but highlight the need for interpretation of any changes in terms of the differential neuropathology involving all relevant white matter fibre tracts.

TBSS allowed us to probe changes across the brain in an unbiased manner. We showed that all indices (FA, MD, MO) exhibited similar patterns of abnormalities when comparing the three groups together (Figs. 2 and 4). Wherever FA was found decreased in the patients (always in a white matter region consisting of one fibre population), MD was increased and MO decreased. Wherever MO was found increased (always in a white matter region consisting of crossing fibres), MD and FA were increased. Increases in MD have often been reported in studies on age- or disease-related neurodegeneration (reviews in Moseley, 2002; Bozzali and Cherubini, 2007; Sullivan and Pfefferbaum, 2006). MD is a sensitive though unspecific marker of degeneration, an increase of MD being likely caused by a decrease in membrane density due to cell degeneration (Beaulieu, 2002). FA and MO give more specific information about the neuropathological process. First, reduced FA is generally interpreted to reflect a decrease in the organisation of the white matter caused by various micro-structural processes such as demyelination, axonal degradation or gliosis (Beaulieu, 2002; Concha et al., 2006; Lebel et al., 2008; Assaf, 2008). As a decrease of MO represents a transition from more linear to more planar shape of the diffusion tensor in white matter, it might therefore also reflect a “disorganisation” of the white matter tracts in the patients. By contrast, the unusual increase of FA – in the context of a neurodegenerative disorder – is likely related to a selective sparing (or selective degeneration) of one of the pathways in a region of crossing fibres (Pierpaoli et al., 2001; Douaud et al., 2009). The co- localised increase of MO in such crossing-fibre region, showing a transition of the white matter to a more linear shape, reinforces this interpretation.

We found in AD a co-localised decrease of FA and MO together with an increase of MD in two tracts carrying cholinergic limbic fibres: the cingulum bundle and the uncinate fasciculus, consistent with previous studies showing reduced FA and increased MD in the cingulum bundle (Bozzali et al., 2002; Fellgiebel et al., 2005; Zhang et al., 2007; Salat et al., 2010) or the uncinate fasciculus (Taoka et al., 2006; Kiuchi et al., 2009). On the other hand, while a reduced FA and/ or an increased MD in the corpus callosum is one of the most consistent findings in AD (Fellgiebel et al., 2004; Stahl et al., 2007), there has been conflicting evidence about whether the genu (Head et al., 2004; Xie et al., 2006) or the splenium (Rose et al., 2000; Takahashi et al., 2002; Medina et al., 2006) shows the greatest neuropathological changes. In our study, we found a decrease in FA and MO accompanied by an increase of MD homogeneously distributed throughout the entire corpus callosum. Diffusion abnormalities in this tract are thought to be a manifestation of Wallerian

degeneration in AD, as shown by correlations between the FA in the corpus callosum and the GM volume in various cortical regions only found in the AD patients (Sydykova et al., 2007). This might explain why corpus callosum abnormalities are rarely found in MCI (Chua et al., 2008; Hess, 2009) as most of the GM volume loss is localised in the medial temporal lobe in MCI (Karas et al., 2004; Hua et al., 2008). Consistent with this, the diffusion differences found between MCI and AD in our study were prominently found in the corpus callosum. Another commissural pathway, the anterior commissure connecting temporal lobe, orbitofrontal cortex and amygdala (Philippon and Baldwin, 1971) showed the same diffusion changes (FA/MO decrease, and MD increase). Interestingly, electron microscopy in aging rhesus monkeys has demonstrated age-related alteration and degeneration of the myelinated fibres in this structure (Sandell and Peters, 2003).

The last tract we found impaired using all indices was the SLF, mainly in the section II of this tract, which extends from the angular gyrus to the caudal-lateral prefrontal regions (Makris et al., 2005). Damage to the SLF II is known to result in disorders of spatial working memory (Preuss and Goldman-Rakic, 1989; Petrides and Pandya, 2002). Decrease of FA and increase of MD in the SLF are consistent with previous findings in AD (Rose et al., 2000; Takahashi et al., 2002; Parente et al., 2008). Remarkably, measures in this tract provided us the only voxel-wise significant differences between healthy elderly and MCI patients, with an MO increase and a co-localised increase of FA found a posteriori. However, it should be noted that we found these significant diffusion abnormalities only in areas where the SLF intersects the projection pathways. Similarly, the only significant differences in correlations (with the Trail-Making test scores) between healthy elderly and MCI patients were found where the SLF crosses the motor-related tracts. It would seem that for the clinically more heterogeneous population of MCI patients (compared with probable AD patients, Ganguli, 2006), considering a subject-specific balance or ratio between spared and affected tracts provides a more sensitive measure than just looking at the affected ones, as it might reduce the variance of the diffusion measures in the affected tracts. Indeed, the quantitative crossing-fibre tractography, that allowed us to probabilistically track both fibre populations, showed unambiguously that the increase of FA, MO and MD was related to a selective sparing of the motor-related tracts compared with the affected SLF. The impact of the disease on diffusion anisotropy measures (FA and MO) is therefore opposite to what one could expect in this region where the affected pathway is the secondary one (with an increase of FA and MO in the patients). On the other hand, regions containing only the SLF merely demonstrated a trend in the diffusion changes between MCI and healthy aging with a more typical decrease of FA and MO decrease (and MD increase). Analogous results have been shown in Huntington's disease, with only a trend in decrease of FA in some known affected tracts but a significant increase of FA when they crossed other pathways in the deep grey matter (Douaud et al., 2009). The relative sparing of the motor pathways in AD, evidenced so far by a lack of significant FA changes (Rose et al., 2000; Bozzali et al., 2002; Takahashi et al., 2002; Kiuchi et al., 2009), is likely reflected by the clinical preservation of the motor functions until later stages of the disease (95% of the AD patients included in this study had mild AD) and is consistent with the preservation of the sensorimotor cortex (Karas et al., 2004; Chetelat et al., 2008; Dickerson et al., 2009).

Europe PMC Funders Author Manuscripts

Conclusions

When investigating in the whole-brain various DTI-derived measures, the only region showing differences between healthy aging and MCI is a region of crossing fibres in the centrum semiovale, with an increased mode of anisotropy explained by a relative sparing of the motor-related pathways compared with the cognitive-related SLF. These findings are likely to explain the opposite direction for correlation with a verbal long term memory test found by Serra and colleagues in crossing-fibre region in AD (Serra et al., 2010) and also provide one plausible explanation for the unexpected increase in axial diffusivity found in two recent studies in AD (Salat et al., 2008; Acosta-Cabronero et al., 2010). As mentioned by the authors of the former study, this result seem indeed in opposition with what is expected from animal models and human corpus callosotomy demonstrating that axonal pathology or transection should result in a decrease in axial diffusivity (Song et al., 2003; Concha et al., 2006). However, in areas of crossing fibres, it is virtually impossible to disentangle axial diffusivity of one of the two fibre populations from the radial diffusivity of the other fibre population (and vice-versa): what these studies have demonstrated might therefore be a degeneration of the second fibre population. Our study highlights a need to interpret diffusion MRI measures of white matter simultaneously in terms of the underlying white matter anatomy and the potential tract-specific neuropathology. As it would seem that grey matter loss in MCI patients compared with healthy controls is mostly confined to the medial temporal lobe and posterior cingulate/precuneus (Whitwell et al., 2008; Hua et al., 2008; Choo et al., 2010), the impairment of the SLF witnessed in crossing fibre regions using the mode of anisotropy might be the evidence of a subtle degeneration not (yet) detected macroscopically in the corresponding grey matter regions. We therefore aim in future work to explore grey matter in the same population to test this hypothesis and to determine with a longitudinal study whether grey matter abnormalities related to our findings in the white matter will emerge. Finally, we believe that the methods used in this study have general applicability for other degenerative disorders and that, beyond the clinical sphere, these methods could contribute to a better understanding and quantification of subtle effects witnessed in normal processes such as visuospatial attention (Tuch et al., 2005) or motor learning (Scholz and Johansen-Berg, 2007, personal communication).

Supplementary Material

Refer to Web version on PubMed Central for supplementary material.

Acknowledgments

The authors are particularly grateful to Drs. Giovanna Zamboni and Nicola Filippini for very helpful comments and discussions. This work was supported by UK Engineering and Physical Sciences Research Council, UK Medical Research Council and the Wellcome Trust for funding. These data were acquired as part of EAGLE, a longitudinal natural history study of Alzheimer's disease conducted at the University of Basel and funded by GlaxoSmithKline (GSK). The authors also acknowledge the invaluable work of Dr. Rachel Gibson in scientific coordination of EAGLE and the close involvement of Ms. Leslie Amos, in coordination of the study and data management. AR, BW and PMM are full-time employees of GSK.

References

Acosta-Cabronero J, Williams GB, Pengas G, Nestor PJ. Absolute diffusivities define the landscape of white matter degeneration in Alzheimer's disease. Brain. 2010 Feb; 133(Pt 2):529–539. [PubMed: 19914928]

American Psychiatric Association. Diagnostic and Statistical Manual of Mental Disorders. 4th edn. American Psychiatric Association; Washington, DC: 1994. 390

Andersson, J; Smith, S; Jenkinson, M. FNIRT — FMRIB's Non-linear Image Registration Tool. Presented at 13th annual meeting of the Organization for Human Brain Mapping (#496); 2008.

Assaf Y. Can we use diffusion MRI as a bio-marker of neurodegenerative processes? Bioessays. 2008 Nov; 30(11–12):1235–1245. [PubMed: 18937377]

Beaulieu C. The basis of anisotropic water diffusion in the nervous system — a technical review. NMR Biomed. 2002 Nov-Dec;15(7–8):435–455. [PubMed: 12489094]

Behrens TE, Berg HJ, Jbabdi S, Rushworth MF, Woolrich MW. Probabilistic diffusion tractography with multiple fibre orientations: what can we gain? Neuroimage. 2007 Jan 1; 34(1):144–155. [PubMed: 17070705]

Bozzali M, Falini A, Franceschi M, Cercignani M, Zuffi M, Scotti G, et al. White matter damage in Alzheimer's disease assessed in vivo using diffusion tensor magnetic resonance imaging. J Neurol Neurosurg Psychiatry. 2002 Jun; 72(6):742–746. [PubMed: 12023417]

Bozzali M, Cherubini A. Diffusion tensor MRI to investigate dementias: a brief review. Magn Reson Imaging. 2007 Jul; 25(6):969–977. [PubMed: 17451903]

Cedazo-Minguez A, Winblad B. Biomarkers for Alzheimer's disease and other forms of dementia: clinical needs, limitations and future aspects. Exp Gerontol. 2010; 45(1):5–14. [PubMed: 19796673]

Chetelat G, Desgranges B, Landeau B, Mezenge F, Poline JB, de la Sayette V, et al. Direct voxel-based comparison between grey matter hypometabolism and atrophy in Alzheimer's disease. 2008 Brain. Jan; 131(Pt 1):60–71. [PubMed: 18063588]

Choo IH, Lee DY, Oh JS, Lee JS, Lee DS, Song IC, et al. Posterior cingulate cortex atrophy and regional cingulum disruption in mild cognitive impairment and Alzheimer's disease. Neurobiol Aging. 2010; 31(5):772–779. [PubMed: 18687503]

Chua TC, Wen W, Slavin MJ, Sachdev PS. Diffusion tensor imaging in mild cognitive impairment and Alzheimer's disease: a review. Curr Opin Neurol. 2008 Feb; 21(1):83–92. [PubMed: 18180656]

Concha L, Gross DW, Wheatley BM, Beaulieu C. Diffusion tensor imaging of time-dependent axonal and myelin degradation after corpus callosotomy in epilepsy patients. Neuroimage. 2006 Sep; 32(3):1090–1099. [PubMed: 16765064]

Douaud G, Behrens TE, Poupon C, Cointepas Y, Jbabdi S, Gaura V, et al. In vivo evidence for the selective subcortical degeneration in Huntington's disease. Neuroimage. 2009 Jul 15; 46(4):958–966. [PubMed: 19332141]

Dickerson BC, Bakkour A, Salat DH, Feczko E, Pacheco J, Greve DN, et al. The cortical signature of Alzheimer's disease: regionally specific cortical thinning relates to symptom severity in very mild to mild AD dementia and is detectable in asymptomatic amyloid-positive individuals. Cereb Cortex. 2009 Mar; 19(3):497–510. [PubMed: 18632739]

Ennis DB, Kindlmann G. Orthogonal tensor invariants and the analysis of diffusion tensor magnetic resonance images. Magn Reson Med. 2006 Jan; 55(1):136–146. [PubMed: 16342267]

Fellgiebel A, Wille P, Muller MJ, Winterer G, Scheurich A, Vucurevic G, et al. Ultrastructural hippocampal and white matter alterations in mild cognitive impairment: a diffusion tensor imaging study. Dement Geriatr Cogn Disord. 2004; 18(1):101–108. [PubMed: 15087585]

Fellgiebel A, Muller MJ, Wille P, Dellani PR, Scheurich A, Schmidt LG, et al. Color-coded diffusion-tensor-imaging of posterior cingulate fiber tracts in mild cognitive impairment. Neurobiol Aging. 2005 Aug-Sep;26(8):1193–1198. [PubMed: 15917103]

Ganguli M. Mild cognitive impairment and the 7 uses of epidemiology. Alzheimer Dis Assoc Disord. 2006 Jul-Sep;20(3) Suppl 2:S52–S57. [PubMed: 16917196]

Gauthier S, Reisberg B, Zaudig M, Petersen RC, Ritchie K, Broich K, et al. Mild cognitive impairment. Lancet. 2006 Apr 15; 367(9518):1262–1270. [PubMed: 16631882]

Grundman M, Petersen RC, Ferris SH, Thomas RG, Aisen PS, Bennett DA, et al. Mild cognitive impairment can be distinguished from Alzheimer disease and normal aging for clinical trials. Arch Neurol. 2004 Jan; 61(1):59–66. [PubMed: 14732621]

Head D, Buckner RL, Shimony JS, Williams LE, Akbudak E, Conturo TE, et al. Differential vulnerability of anterior white matter in nondemented aging with minimal acceleration in dementia of the Alzheimer type: evidence from diffusion tensor imaging. Cereb Cortex. 2004 Apr; 14(4):410–423. [PubMed: 15028645]

Hess CP. Update on diffusion tensor imaging in Alzheimer's disease. Magn Reson Imaging Clin N Am. 2009 May; 17(2):215–224. [PubMed: 19406355]

Hua X, Leow AD, Parikshak N, Lee S, Chiang MC, Toga AW, et al. Tensor-based morphometry as a neuroimaging biomarker for Alzheimer's disease: an MRI study of 676 AD, MCI, and normal subjects. Neuroimage. 2008 Nov 15; 43(3):458–469. [PubMed: 18691658]

Karas GB, Scheltens P, Rombouts SA, Visser PJ, van Schijndel RA, Fox NC, et al. Global and local gray matter loss in mild cognitive impairment and Alzheimer's disease. Neuroimage. 2004 Oct; 23(2):708–716. [PubMed: 15488420]

Kier EL, Staib LH, Davis LM, Bronen RA. MR imaging of the temporal stem: anatomic dissection tractography of the uncinate fasciculus, inferior occipitofrontal fasciculus, and Meyer's loop of the optic radiation. AJNR Am J Neuroradiol. 2004 May; 25(5):677–691. [PubMed: 15140705]

Kiuchi K, Morikawa M, Taoka T, Nagashima T, Yamauchi T, Makinodan M, et al. Abnormalities of the uncinate fasciculus and posterior cingulate fasciculus in mild cognitive impairment and early Alzheimer's disease: a diffusion tensor tractography study. Brain Res. 2009 Sep 1.1287:184–191. [PubMed: 19559010]

Lebel C, Walker L, Leemans A, Phillips L, Beaulieu C. Microstructural maturation of the human brain from childhood to adulthood. Neuroimage. 2008 Apr 15; 40(3):1044–1055. [PubMed: 18295509]

Liu Y, Spulber G, Lehtimäki KK, Könönen M, Hallikainen I, Gröhn H, Kivipelto M, Hallikainen M, Vanninen R, Soininen H. Diffusion tensor imaging and Tract-Based Spatial Statistics in Alzheimer's disease and mild cognitive impairment. Neurobiol Aging. 2009 Nov 11.

McKhann G, Drachman D, Folstein M, Katzman R, Price D, Stadlan EM. Clinical diagnosis of Alzheimer's disease: report of the NINCDS-ADRDA Work Group under the auspices of Department of Health and Human Services Task Force on Alzheimer's Disease. Neurology. 1984 Jul; 34(7):939–944. [PubMed: 6610841]

Makris N, Kennedy DN, McInerney S, Sorensen AG, Wang R, Caviness VS Jr, et al. Segmentation of subcomponents within the superior longitudinal fascicle in humans: a quantitative, in vivo, DT-MRI study. Cereb Cortex. 2005 Jun; 15(6):854–869. [PubMed: 15590909]

Medina D, DeToledo-Morrell L, Urresta F, Gabrieli JD, Moseley M, Fleischman D, et al. White matter changes in mild cognitive impairment and AD: a diffusion tensor imaging study. Neurobiol Aging. 2006 May; 27(5):663–672. [PubMed: 16005548]

Moseley M. Diffusion tensor imaging and aging — a review. NMR Biomed. 2002 Nov-Dec;15(7–8):553–560. [PubMed: 12489101]

Nichols TE, Holmes AP. Nonparametric permutation tests for functional neuroimaging: a primer with examples. Hum Brain Mapp. 2002 Jan; 15(1):1–25. [PubMed: 11747097]

Parente DB, Gasparetto EL, da Cruz LC Jr, Domingues RC, Baptista AC, Carvalho AC. Potential role of diffusion tensor MRI in the differential diagnosis of mild cognitive impairment and Alzheimer's disease. AJR Am J Roentgenol. 2008 May; 190(5):1369–1374. [PubMed: 18430857]

Petersen RC, Thomas RG, Grundman M, Bennett D, Doody R, Ferris S, et al. Vitamin E and donepezil for the treatment of mild cognitive impairment. N Engl J Med. 2005 Jun 9; 352(23):2379–2388. [PubMed: 15829527]

Petersen RC. Early diagnosis of Alzheimer's disease: is MCI too late? Curr Alzheimer Res. 2009 Aug; 6(4):324–330. [PubMed: 19689230]

Petrides, M, Pandya, DN. Association pathways of the prefrontal cortex and functional observations. In: Struss, DT, Knight, RT, editors. Principles of Frontal Lobe Function. Oxford University Press; Oxford: 2002. 31–50.

Philippon J, Baldwin M. Role of the anterior commissure in the contralateral propagation of the after-discharge from amygdala and temporal cortex in the monkey. Acta Neurochirurgica. 1971; 23(4):311–323.

Pierpaoli C, Barnett A, Pajevic S, Chen R, Penix LR, Virta A, et al. Water diffusion changes in Wallerian degeneration and their dependence on white matter architecture. Neuroimage. 2001 Jun; 13(6) Pt 1:1174–1185. [PubMed: 11352623]

Preuss TM, Goldman-Rakic PS. Connections of the ventral granular frontal cortex of macaques with perisylvian premotor and somatosensory areas: anatomical evidence for somatic representation in primate frontal association cortex. J Comp Neurol. 1989 Apr 8; 282(2):293–316. [PubMed: 2708598]

Rose SE, Chen F, Chalk JB, Zelaya FO, Strugnell WE, Benson M, et al. Loss of connectivity in Alzheimer's disease: an evaluation of white matter tract integrity with colour coded MR diffusion tensor imaging. J Neurol Neurosurg Psychiatry. 2000 Oct; 69(4):528–530. [PubMed: 10990518]

Rose SE, McMahon KL, Janke AL, O'Dowd B, de Zubicaray G, Strudwick MW, et al. Diffusion indices on magnetic resonance imaging and neuropsychological performance in amnestic mild cognitive impairment. J Neurol Neurosurg Psychiatry. 2006 Oct; 77(10):1122–1128. [PubMed: 16754694]

Salat DH, Tuch DS, van der Kouwe AJ, Greve DN, Pappu V, Lee SY, et al. White matter pathology isolates the hippocampal formation in Alzheimer's disease. Neurobiol Aging. 2010; 31(2):244–256. [PubMed: 18455835]

Sandell JH, Peters A. Disrupted myelin and axon loss in the anterior commissure of the aged rhesus monkey. J Comp Neurol. 2003 Nov 3; 466(1):14–30. [PubMed: 14515238]

Scholz J, Johansen-Berg H. Individual differences in complex motor task performance correlate with white matter integity in specific regions of the motor system. Presented at 13th annual meeting of the Organization for Human Brain Mapping. 2007

Serra L, Cercignani M, Lenzi D, Perri R, Fadda L, Caltagirone C, et al. Grey and white matter changes at different stages of Alzheimer's disease. J Alzheimers Dis. 2010 Jan; 19(1):147–159. [PubMed: 20061634]

Smith SM, Jenkinson M, Woolrich MW, Beckmann CF, Behrens TE, Johansen-Berg H, et al. Advances in functional and structural MR image analysis and implementation as FSL. Neuroimage. 2004; 23(Suppl 1):S208–S219. [PubMed: 15501092]

Smith SM, Jenkinson M, Johansen-Berg H, Rueckert D, Nichols TE, Mackay CE, et al. Tract-based spatial statistics: voxelwise analysis of multi-subject diffusion data. Neuroimage. 2006 Jul 15; 31(4):1487–1505. [PubMed: 16624579]

Smith SM, Nichols TE. Threshold-free cluster enhancement: addressing problems of smoothing, threshold dependence and localisation in cluster inference. Neuroimage. 2009 Jan 1; 44(1):83–98. [PubMed: 18501637]

Song SK, Sun SW, Ju WK, Lin SJ, Cross AH, Neufeld AH. Diffusion tensor imaging detects and differentiates axon and myelin degeneration in mouse optic nerve after retinal ischemia. Neuroimage. 2003 Nov; 20(3):1714–1722. [PubMed: 14642481]

Stahl R, Dietrich O, Teipel SJ, Hampel H, Reiser MF, Schoenberg SO. White matter damage in Alzheimer disease and mild cognitive impairment: assessment with diffusion-tensor MR imaging and parallel imaging techniques. Radiology. 2007 May; 243(2):483–492. [PubMed: 17456872]

Stricker NH, Schweinsburg BC, Delano-Wood L, Wierenga CE, Bangen KJ, Haaland KY, et al. Decreased white matter integrity in late-myelinating fiber pathways in Alzheimer's disease supports retrogenesis. Neuroimage. 2009 Mar 1; 45(1):10–16. [PubMed: 19100839]

Sullivan EV, Pfefferbaum A. Diffusion tensor imaging and aging. Neurosci Biobehav Rev. 2006; 30(6):749–761. [PubMed: 16887187]

Sydykova D, Stahl R, Dietrich O, Ewers M, Reiser MF, Schoenberg SO, et al. Fiber connections between the cerebral cortex and the corpus callosum in Alzheimer's disease: a diffusion tensor imaging and voxel-based morphometry study. Cereb Cortex. 2007 Oct; 17(10):2276–2282. [PubMed: 17164468]

Takahashi S, Yonezawa H, Takahashi J, Kudo M, Inoue T, Tohgi H. Selective reduction of diffusion anisotropy in white matter of Alzheimer disease brains measured by 3.0 Tesla magnetic resonance imaging. Neurosci Lett. 2002 Oct 25; 332(1):45–48. [PubMed: 12377381]

Taoka T, Iwasaki S, Sakamoto M, Nakagawa H, Fukusumi A, Myochin K, et al. Diffusion anisotropy and diffusivity of white matter tracts within the temporal stem in Alzheimer disease: evaluation of the "tract of interest" by diffusion tensor tractography. AJNR Am J Neuroradiol. 2006 May; 27(5):1040–1045. [PubMed: 16687540]

Teipel SJ, Stahl R, Dietrich O, Schoenberg SO, Perneczky R, Bokde AL, et al. Multivariate network analysis of fiber tract integrity in Alzheimer's disease. Neuroimage. 2007 Feb 1; 34(3):985–995. [PubMed: 17166745]

Tuch DS, Salat DH, Wisco JJ, Zaleta AK, Hevelone ND, Rosas HD. Choice reaction time performance correlates with diffusion anisotropy in white matter pathways supporting visuospatial attention. Proc Natl Acad Sci USA. 2005 Aug 23; 102(34):12212–12217. [PubMed: 16103359]

Wedeen VJ, Wang RP, Schmahmann JD, Benner T, Tseng WY, Dai G, et al. Diffusion spectrum magnetic resonance imaging (DSI) tractography of crossing fibers. Neuroimage. 2008 Jul 15; 41(4):1267–1277. [PubMed: 18495497]

Whitwell JL, Shiung MM, Przybelski SA, Weigand SD, Knopman DS, Boeve BF, et al. MRI patterns of atrophy associated with progression to AD in amnestic mild cognitive impairment. Neurology. 2008 Feb 12; 70(7):512–520. [PubMed: 17898323]

Winblad B, Palmer K, Kivipelto M, Jelic V, Fratiglioni L, Wahlund LO, et al. Mild cognitive impairment—beyond controversies, towards a consensus: report of the International Working Group on Mild Cognitive Impairment. J Intern Med. 2004 Sep; 256(3):240–246. [PubMed: 15324367]

Xie S, Xiao JX, Gong GL, Zang YF, Wang YH, Wu HK, et al. Voxel-based detection of white matter abnormalities in mild Alzheimer disease. Neurology. 2006; 66(1):1845–1849. [PubMed: 16801648]

Zhang Y, Schuff N, Jahng GH, Bayne W, Mori S, Schad L, et al. Diffusion tensor imaging of cingulum fibers in mild cognitive impairment and Alzheimer disease. Neurology. 2007 Jan 2; 68(1):13–19. [PubMed: 17200485]

Europe PMC Funders Author Manuscripts

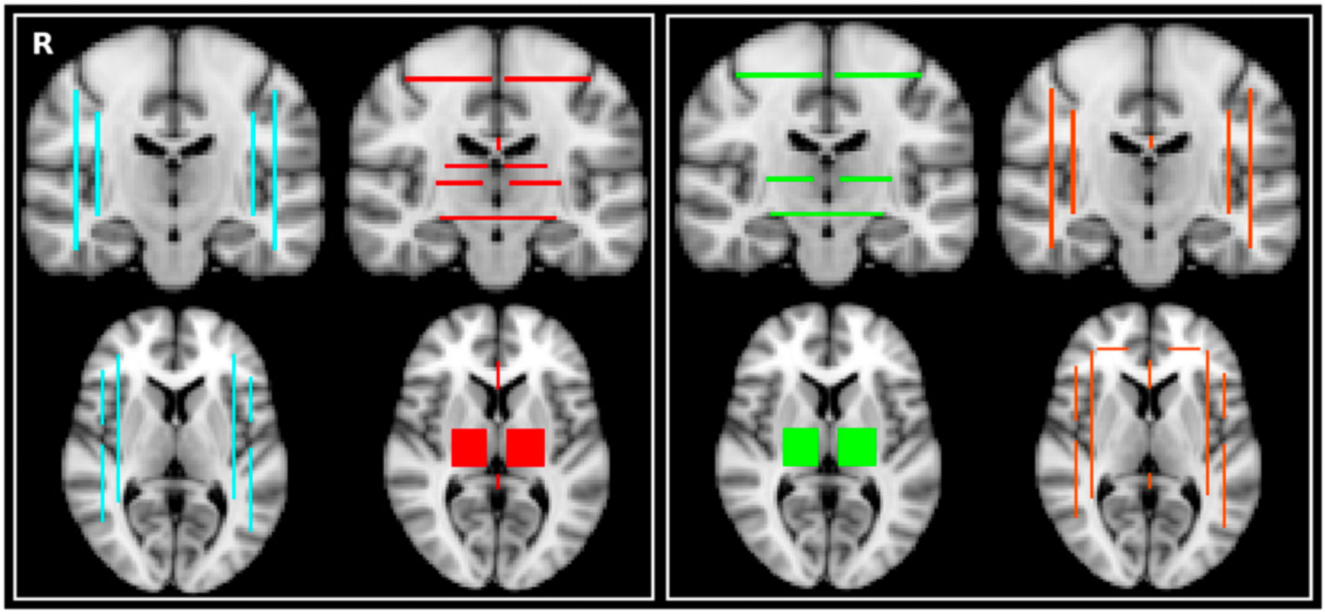

Fig. 1.

Left. Target mask (turquoise) and exclusion mask (red) for the association fibres (AF). Right. Target mask (green) and exclusion mask (orange) for the projections fibres (PF).

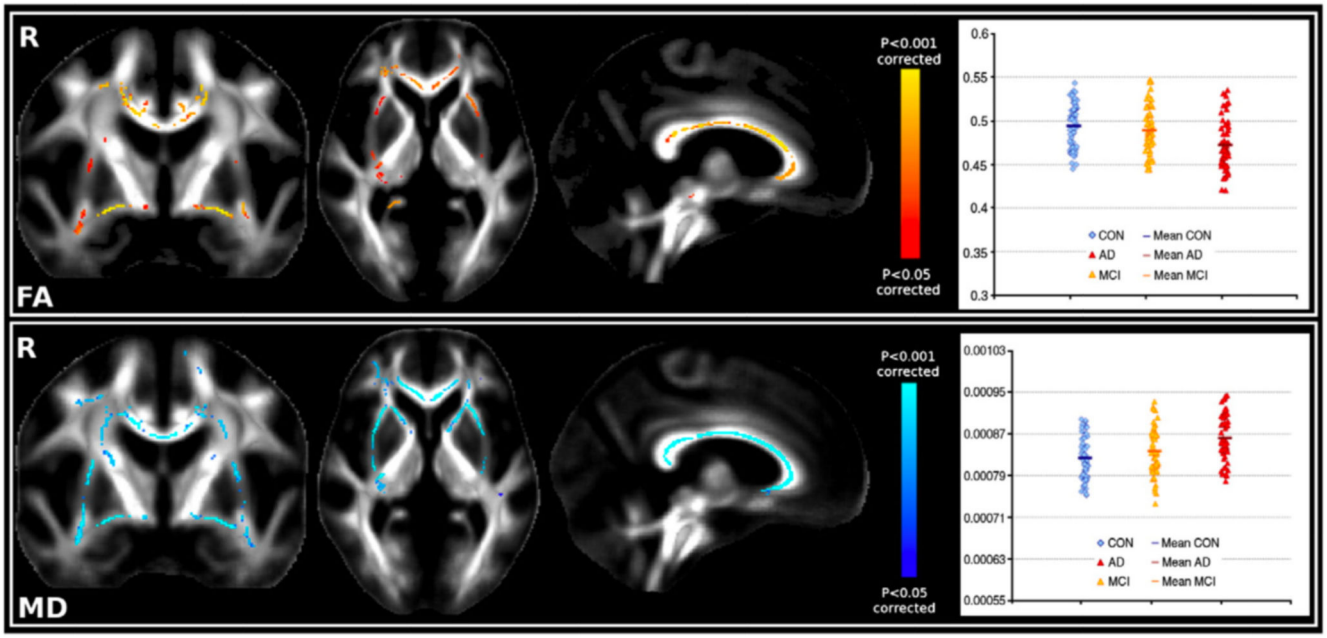

Fig. 2.

Top. Significant FA differences (F-test) across the 3 groups; Plot: FA values in the significant TBSS FA regions highlighted in the figure. Bottom. Significant MD differences (F-test) across the 3 groups; Plot: MD values in the significant TBSS MD regions highlighted in the figure.

Europe PMC Funders Author Manuscripts

Europe PMC Funders Author Manuscripts

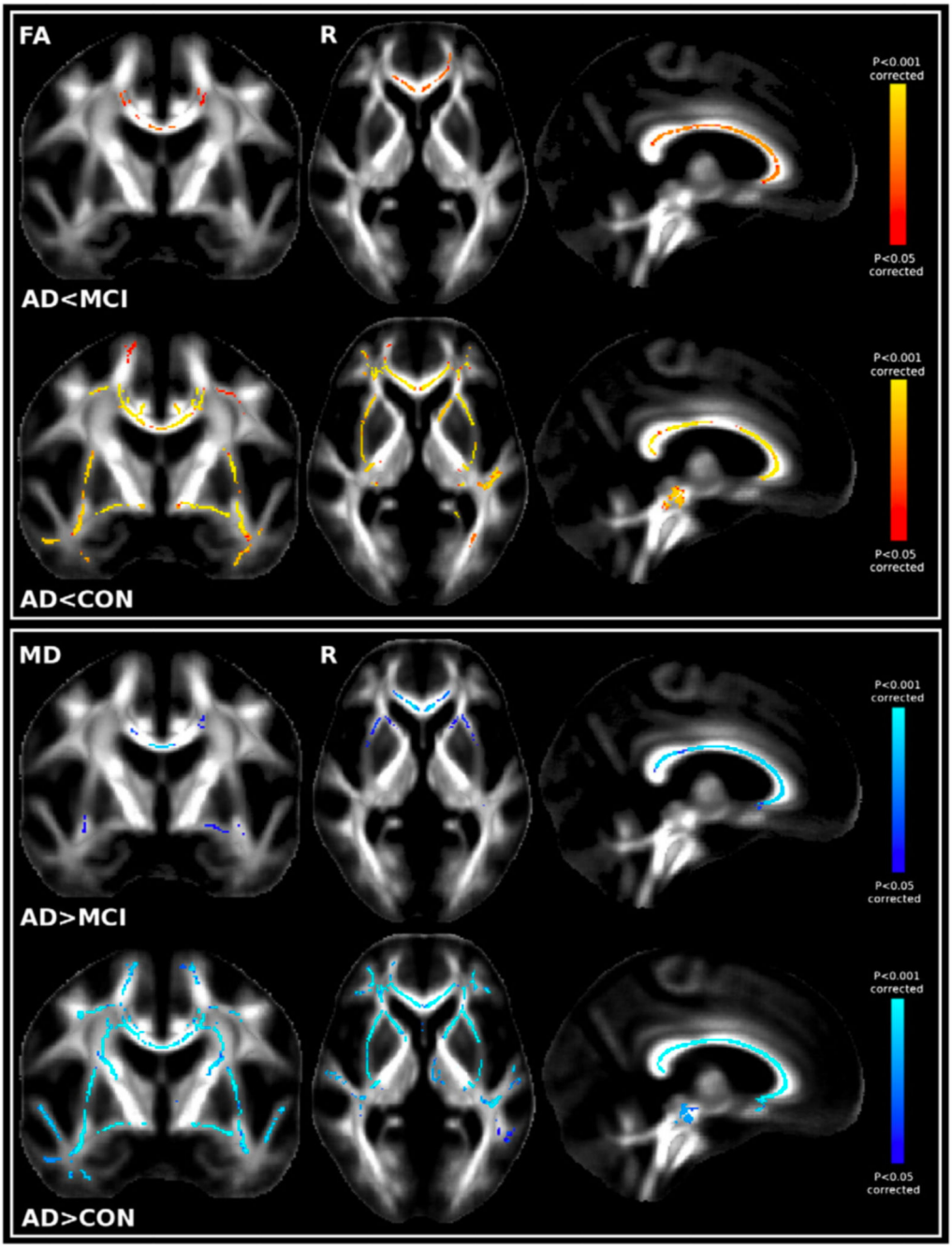

Fig. 3.

Top. First row: Significant TBSS FA results showing the contrast MCI N AD; Second row: Significant TBSS FA results showing CON N AD. Bottom. First row: Significant TBSS MD results showing the contrast ADNMCI; Second row: Significant TBSS MD results showing ADNCON. No significant differences between CON and MCI were found with either FA or MD.

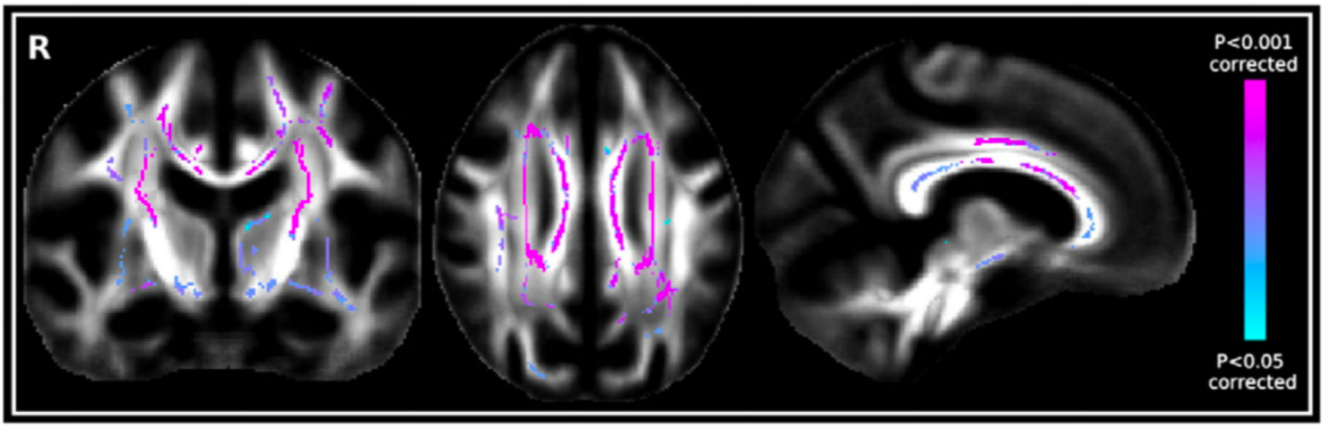

Fig. 4.
Significant TBSS MO differences (F-test) across the 3 groups.

Europe PMC Funders Author Manuscripts

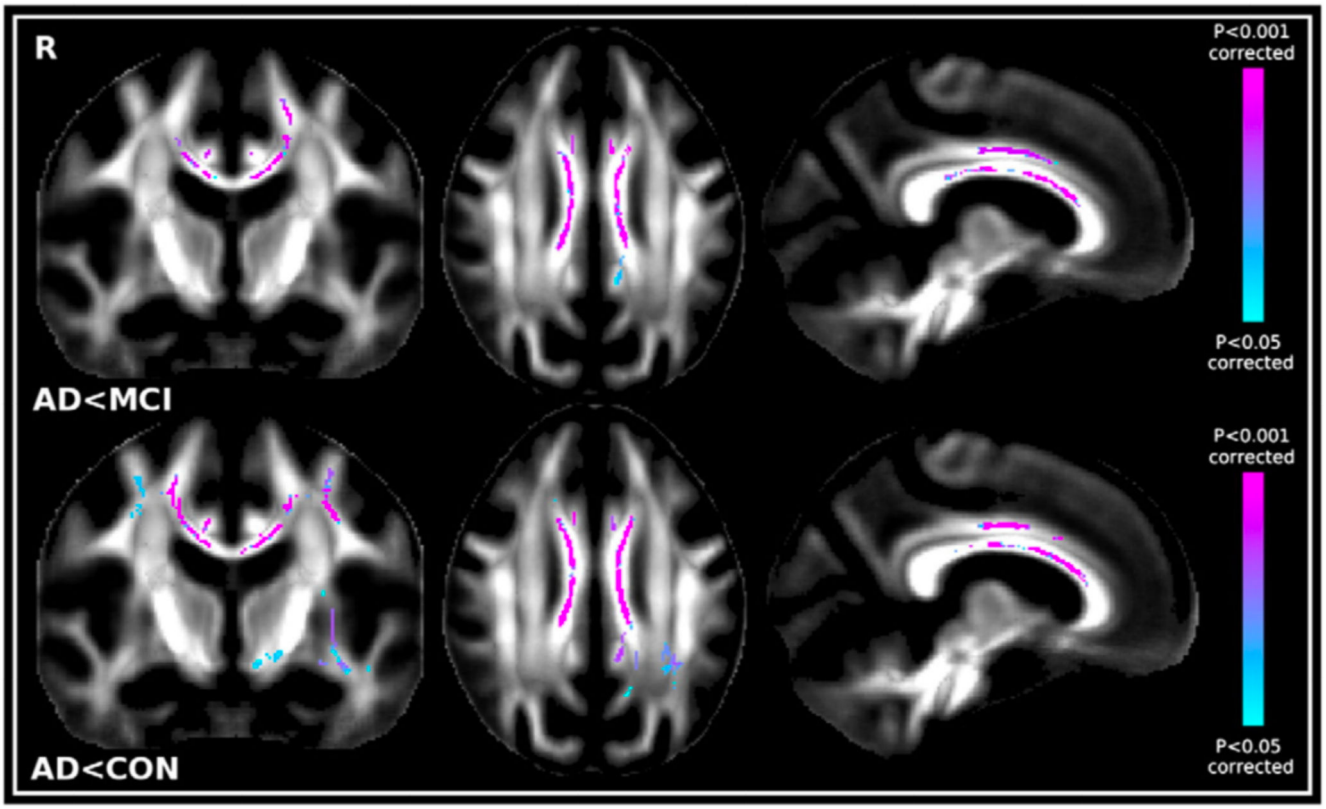

Fig. 5.

Top. Significant TBSS MO results showing the contrast MCINAD. Bottom. Significant TBSS MO results showing CONNAD.

Europe PMC Funders Author Manuscripts

Europe PMC Funders Author Manuscripts

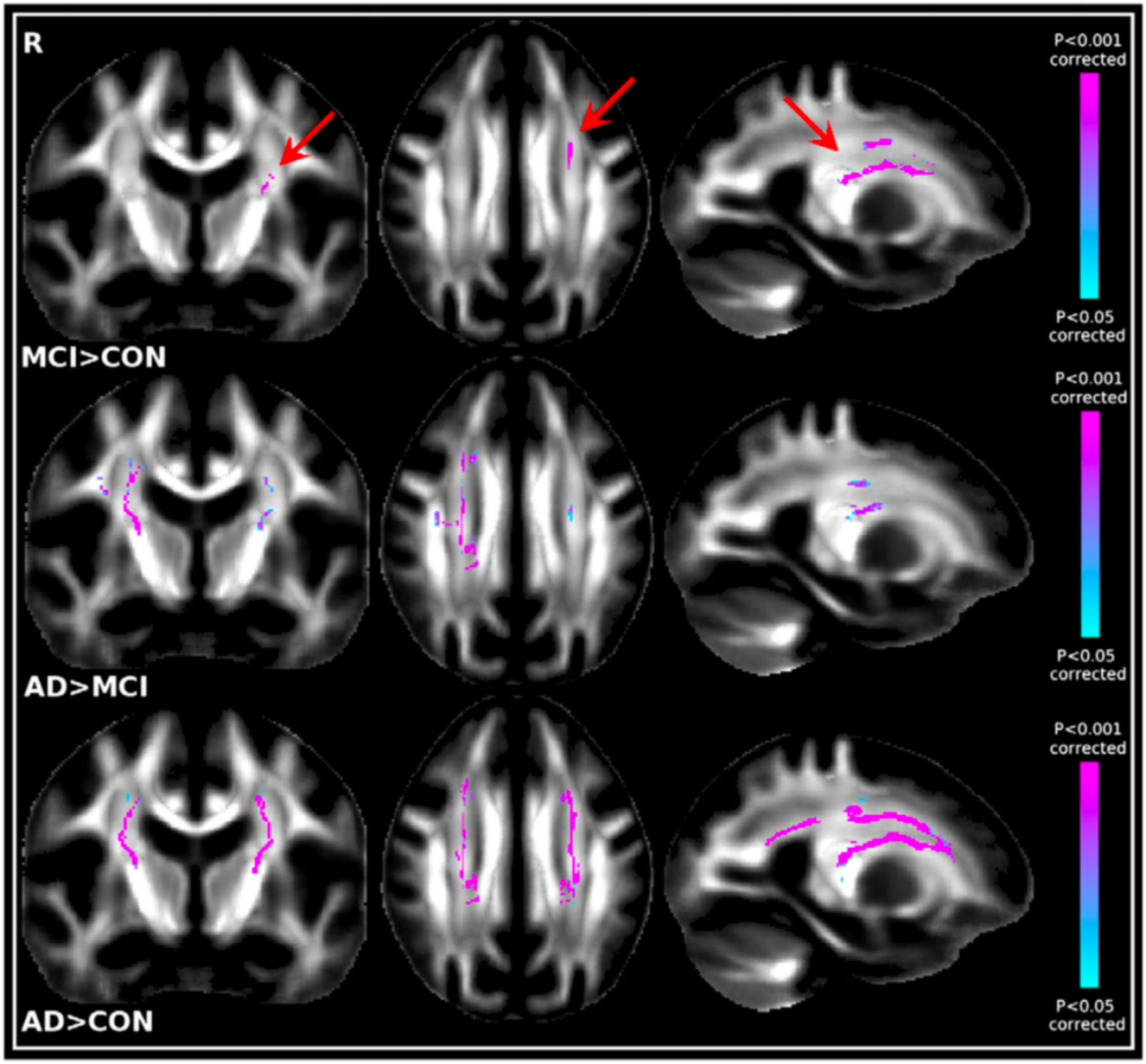

Fig. 6.

Top. Significant TBSS MO results showing the contrast MCINCON (arrows). Middle. Significant TBSS MO results showing the contrast ADNMCI. Bottom. Significant TBSS MO results showing the contrast ADNCON.

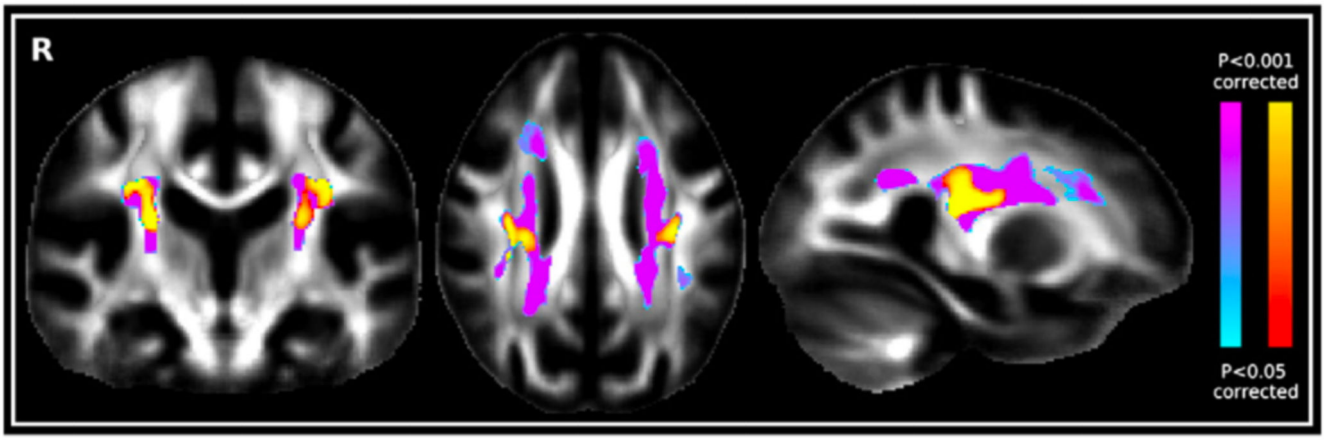

Fig. 7.
Significant voxel-wise increase of FA in AD compared with healthy controls (red–yellow) superimposed over the voxel-wise increase of MO in AD compared with controls (blue–pink).

Europe PMC Funders Author Manuscripts

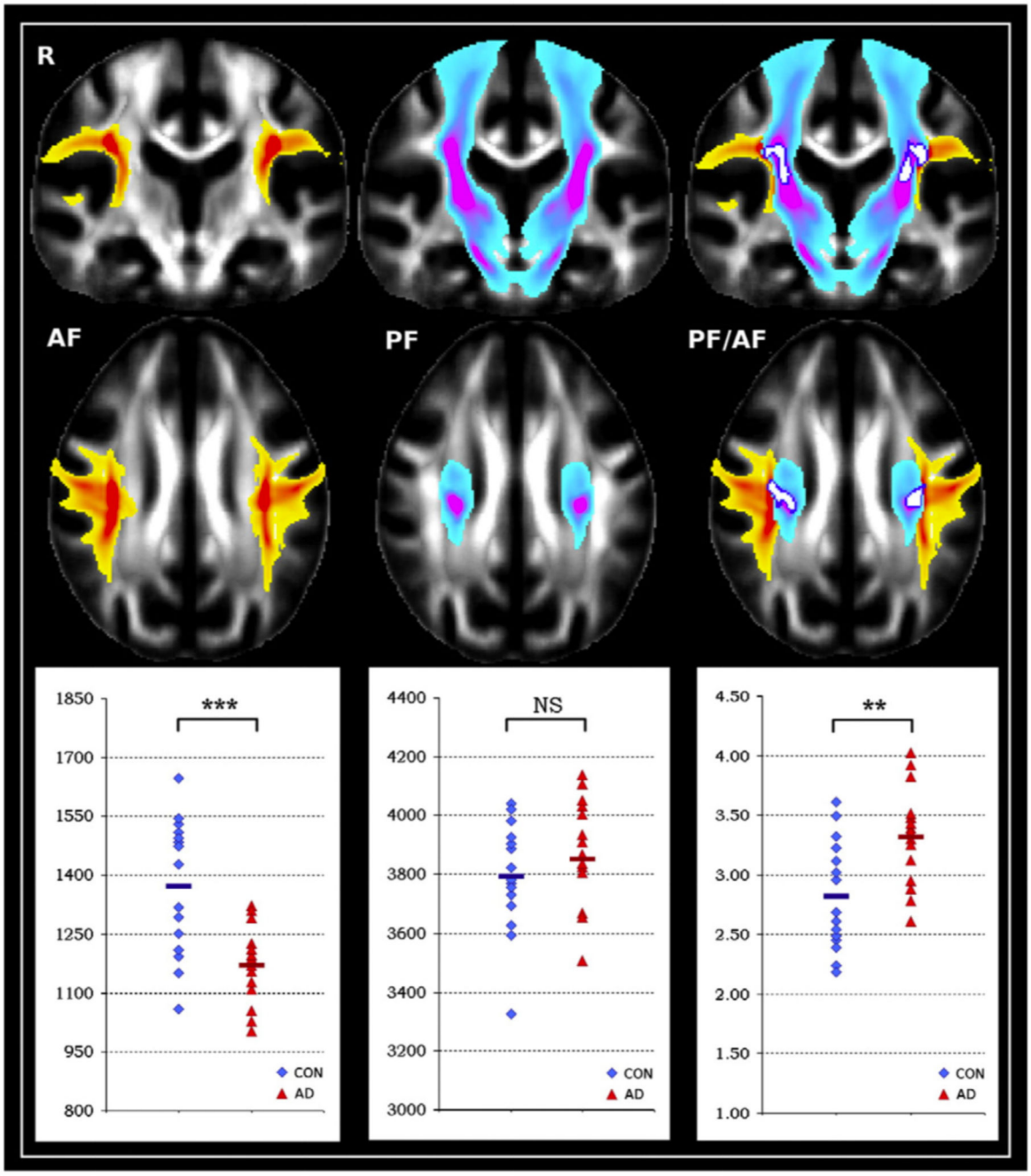

Fig. 8.

Left. Average result of the tracing of the association fibres (AF; yellow–red); boxplot shows average number of particles belonging to the association fibres (***P = 0.0002). Middle. The tracing of the projection fibres (PF: blue–pink) and average number of particles belonging to the projection fibres (NS: non-significant). Right. Seed mask region (white, dark blue contours) over both association and projection fibres results of the tracing; boxplot

shows ratio of the number of particles belonging to the projection fibres over the association fibres (**P=0.002).

Europe PMC Funders Author Manuscripts

Table 1

White matter tracts	FA	MD	MO
F-test across the three groups			
External/extreme capsule/temporal stem	√	√	√
Corpus callosum	√	√	√
Anterior commissure	√	√	√
Cingulum bundle	√	√	√
Anterior thalamic radiations	X	√	√
Superior longitudinal fasciculus	√	√	√
Centrum semi-ovale	√	√	√
	√	√	√
t-test between CON and AD			
External/extreme capsule/temporal stem	+	−	+
Corpus callosum	+	−	+
Anterior commissure	+	−	+
Cingulum bundle	+	−	+
Anterior thalamic radiations	+	−	X
Superior longitudinal fasciculus	+	−	+
Centrum semi-ovale	X	−	−
t-test between MCI and AD			
Corpus callosum	+	−	+
Cingulum bundle	+	−	+
Centrum semi-ovale	X	X	−
t-test between CON and MCI			
Centrum semi-ovale	X	X	−

Summary of the results obtained with TBSS on all three diffusion indices. √ = significant result; X = no significant result; + = significant result in the contrast group 1Ngroup 2; − = significant result in the contrast group 1bgroup 2.